Transmission resonance in an infinite strip of phason defects of a Penrose approximant network

1995 J. Phys.: Condens. Matter 7 8883

(http://iopscience.iop.org/0953-8984/7/47/009)

J. Phys.: Condens. Matter 7 (1995) 8883–8896. Printed in the UK

Transmission resonance in an infinite strip of phason defects of a Penrose approximant network

K Moulopoulos and S Roche
Laboratoire d'Etudes des Propriétés Electronique des Solides, CNRS, 38042 Grenoble, France

Received 23 May 1995

Abstract. An exact method that analytically provides transfer matrices in finite networks of quasicrystalline approximants of any dimensionality is discussed. We use these matrices in two ways: (a) to exactly determine the band structure of an infinite approximant network in analytical form; (b) to determine, also analytically, the quantum resistance of a finite strip of a network under appropriate boundary conditions. As a result of a subtle interplay between topology and phase interferences, we find that a strip of phason defects along a special symmetry direction of a low 2D Penrose approximant, leads to the rigorous vanishing of the reflection coefficient for certain energies. A similar behaviour appears in a low 3D approximant. This type of 'resonance' is discussed in connection with the gap structure of the corresponding ordered (undefected) system.

1. Introduction

Recent experimental work [1] shows that quasicrystals and quasicrystalline approximants have curious (for metallic materials) transport properties. Anomalously high values of the low-temperature resistivity, and the resistivity decrease with the introduction of defects or with an increase of temperature, are typical examples. We have recently analysed [2] the role of a particular type of phason defect on the conductance of a Fibonacci chain. From a consideration of the scattering problem of non-interacting electrons through the chain we have demonstrated subtle interference effects between the hyperspace construction and the phase coherence of the wavefunctions in real space. A full continuous formulation (as opposed to usual discretized approximations of a tight-binding form) was critical [2] for obtaining these interferences, i.e. the full phase coherence had to be kept without truncation approximations. Motivated by that work, here we follow a similar continuous scattering formalism, but in model systems of higher dimensionality.

Within a continuous approach, a way to study structural aspects in higher dimensionality *exactly*, is to treat *networks* of wires [3] that form a particular 2D or 3D structure. The electrons can propagate only along the wires, but their wavefunctions *split* at every vertex by respecting continuity and quantum-mechanical current conservation at every vertex. (This splitting is the analogue of scattering in the full high-dimension problem.) These are good (exactly soluble) model systems that can show non-trivial interference effects on the phase of the exact wavefunctions, and that can also demonstrate how these are affected by the particular topology (manifested by the connectivities characterizing the selected structure).

Our goal here is to study such structural effects on phase interferences, but also to see *how* these are influenced by the introduction of *defects* in the structure, in the form of disruption of long-range order. We find a type of resonance upon introduction of a particular

0953-8984/95/478883+14$19.50

kind of defect, which is the result of a subtle interplay between phase interferences and the topology introduced by the defect.

The structures used can be periodic, but with non-trivial unit cells. Periodicity combined with the scattering formalism leads to a natural study of quasicrystalline approximants. We should emphasize that consideration of such a scattering (or equivalently, transmission) problem, gives *full* information on the states and the spectrum. The band structure of these approximants can be given exactly in closed form (with the coupling of modes in different directions kept in full without approximations). These are therefore good textbook examples of derivations of band structures in high dimensionality, by simply starting from a scattering problem through a single unit cell.

The defects introduced are of a phason-type (but different from the ones studied in [2]) and in real space they correspond to *flips* of the internal structure of the unit cell. Our goal is to study the influence of such a flip on the transmission properties. We actually find, as already mentioned, at least one system where the flipping causes a rigorous vanishing of backscattering (reflection coefficient) for some incidence energies. Introduction of an infinite strip of such flippings leads to a 'resonance', while introduction of a finite number of them lowers the resistance of an otherwise ordered strip. Although these results are rigorous for a strip of unit cells under some special type of boundary conditions, comparison with the same method applied to a square lattice gives evidence that this vanishing may be related to the creation of some extended states in the infinite lattice upon introduction of flipping. This observation may be seen as a manifestation of anomalous transmission behaviour, consistent with numerical works [4] on 2D Penrose lattices (in a tight-binding approximation), and also in general agreement with experiments [1] in real approximants. We also find that the special energies where the resonance occurs lie in the middle of gaps of the infinite (undefected) approximant. We propose this as evidence that a possible creation of extended states may be due to the creation of levels (upon flipping) in gaps of the ordered system.

2. The method

We solve the full continuous and static Schrödinger equation in each branch (wire) of the network. No truncation approximations are made, so that the full phase coherence of the wavefunctions is maintained. For simplicity, we use a vanishing potential along each wire (free electrons along each branch) and take the length of each branch as a common length (l) (however we can still form various non-trivial structures by connecting the wires appropriately, see for example figure 3). For more complicated treatments (i.e. for effects of disorder by introducing random potentials along the wires, etc) the above assumptions can of course be relaxed.

We then match the solutions from all wires that join at a point (vertex): continuity of the wavefunction and quantum-mechanical current conservation at each vertex are enforced [3]. The method is formally similar to discussions [5] of the linearized Ginzburg–Landau equation in superconducting networks.

We give for example the matching equations for the simplest single-vertex arrangements shown in figure 1.

For case (a) of three wires we have

$$A_1 e^{ikl} + B_1 e^{-ikl} = A_1' + B_1' = A_0 + B_0 \tag{1}$$

from the continuity of the wavefunctions, and

$$A_1 e^{ikl} - B_1 e^{-ikl} = A_1' - B_1' + A_0 - B_0 \tag{2}$$

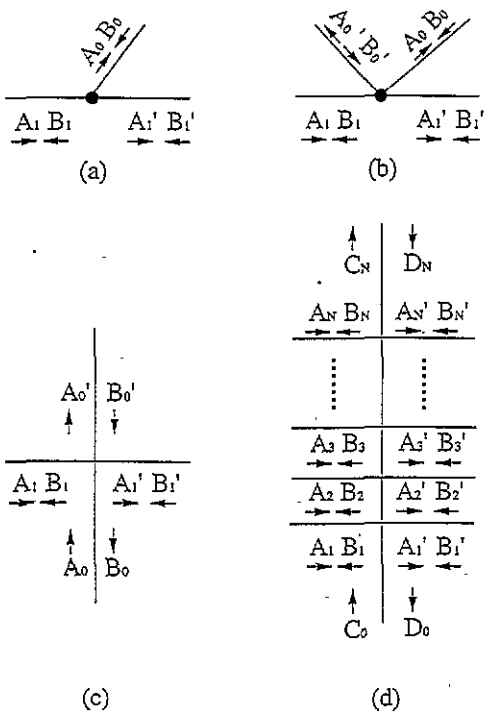

Figure 1. (*a*) The simplest single-vertex arrangement, with branch 1 being viewed as the input, 1′ as the output, and 0 as the 'transverse' branch. (*b*) The single vertex with two transverse branches 0 and 0′. (*c*) The elementary vertex for the square network problem. (*d*) The multi-vertex arrangement for a finite square network.

as one way to assure quantum-mechanical current conservation. In the above, A and B are the coefficients of the two linearly independent plane waves (with wavevector k) along each wire.

A 2×2 transfer matrix can be defined that describes the scattering of electrons incident at branch 1 and transmitted at branch 1′, while branch 0 is viewed as the 'transverse' escape of electrons. If, for example, we look at a situation where electrons are *not* incident from outside through branch 0 (which is equivalent to setting $B_0 = 0$), but they can *only* escape through this branch (i.e. $A_0 \neq 0$), then elimination of A_0 from equations (1) and (2) leads to

$$\begin{pmatrix} A_1' \\ B_1' \end{pmatrix} = \frac{1}{2} \begin{pmatrix} e^{ikl} & -e^{-ikl} \\ e^{ikl} & 3e^{-ikl} \end{pmatrix} \begin{pmatrix} A_1 \\ B_1 \end{pmatrix} \tag{3}$$

which defines the 2×2 transfer matrix for this simplest possible case (the determinant of this matrix is 1, as expected, from the conservation of probability).

It is important to emphasize that the topology of the selected structure (manifested by the corresponding connectivity of the wires) is crucial for the *form* of the resulting matrices. To show this, let us also determine the 2×2 transfer matrix associated with case (b), with two transverse channels, of figure 1. For this case, the matching equations are

$$A_1 e^{ikl} + B_1 e^{-ikl} = A_1' + B_1' = A_0 + B_0 = A_0' + B_0' \tag{4}$$

from the continuity of the wavefunctions, and

$$A_1 e^{ikl} - B_1 e^{-ikl} = A_1' - B_1' + A_0 - B_0 + A_0' - B_0' \tag{5}$$

from current conservation. Once again, if we treat branch 1 as the input branch, 1′ as the output branch, and 0 and 0′ as free transverse escapes (i.e. we impose $B_0 = B_0' = 0$, i.e. no

additional input of electrons from the transverse directions, but *only* output that is naturally determined from the Schrödinger equation), then elimination of A_0 and A_0' from equations (4) and (5) leads to

$$\begin{pmatrix} A_1' \\ B_1' \end{pmatrix} = \begin{pmatrix} 0 & -e^{-ikl} \\ e^{ikl} & 2e^{-ikl} \end{pmatrix} \begin{pmatrix} A_1 \\ B_1 \end{pmatrix}. \tag{6}$$

Note that the 2×2 transfer matrix for this case is different from (3), the sole reason being the fact that there is one *additional* transverse channel compared to case (a). (However the determinant of (6) is also 1, as expected.)

We conclude from these trivial (single-vertex) cases, that the topology (connectivity) is *very* important for the form of the transfer matrices (and hence of any transmission properties, as, for example, the resistance (see below)). The selected topology actually leads to non-trivial forms for the transfer matrices and the transmission properties, as will be discussed below.

It is important to note that even for a complex problem (of many wires and many vertices forming a particular structure, as will be shown below, see figure 3) it is always legitimate to choose one wire as the input channel and any other wire as the output one, with all the rest as 'outside' wires (i.e. lying to the exterior of the chosen unit), treated as transverse escape-channels, irrespective of their number. (In the interior of the selected unit, *everything* (even closed loops) is accounted for in an exact manner through the splitting of the wavefunction *everywhere* (in *all* vertices). Therefore, the topology of the particular structure chosen affects very sensitively the resulting transmission properties, see below.) By then choosing boundary conditions of some type for the coefficients in these external transverse wires, we can always obtain a 2×2 transfer matrix, as above, but, in general, with elements that can be quite complicated functions of kl, the form of which depends on the topology of the selected structure (of *both* internal *and* external connectivities) and describes the complete phase coherence throughout the selected unit. This will be done in the following sections.

Let us first, however, use the concept of the transfer matrix, as introduced above, to discuss transmission properties. Usually, for a complex system with many channels, one speaks in terms of the multi-channel Landauer formula [6] in order to define a measure of the resistance. Here, however, we find it more convenient to focus on the channels that we choose as input and output branches, and to define an *effective* resistance, even in the presence of the transverse escapes. By making a small modification (see the Appendix) to the standard Landauer argument [7] we find that this effective resistance is given, for spin-$\frac{1}{2}$ electrons, by

$$\mathcal{R} = \frac{\pi\hbar}{e^2} \frac{(R - T + 1)}{2(1 - R)} \tag{7}$$

with R and T the (partial) reflection and transmission coefficients resulting from the 2×2 transfer matrix (as discussed above) of the problem under consideration. It turns out that these coefficients are given by the elements of the transfer matrix ($\hat{T}$) as follows

$$R = \frac{|T_{21}|^2}{|T_{22}|^2} \tag{8}$$

and

$$T = \frac{1}{|T_{22}|^2}. \tag{9}$$

Note that (7) yields the usual Landauer ratio R/T if there are no transverse escapes or if periodicity is enforced in the transverse channels (or generally whenever $R + T = 1$ is valid).

The boundary conditions (for the transverse wires) that we use in what follows are of two types: one might be called 'free scattering' and correspond to vanishing transverse incidence (as the ones used in the above trivial single-vertex cases), and the other is periodic boundary conditions in the transverse directions. The latter can lead to band structures, as will be seen below. But a link between the two types is expected, as we now discuss in the case of the simplest 2D structure: a square network.

3. Example: a square lattice

3.1. The transmission problem

The basic vertex problem to be solved is shown in figure 1(*d*). Matching the solution in all N vertices results in transfer matrices, with forms depending on the boundary conditions.

(i) For 'free scattering', namely $C_0 = D_N = 0$ (no current input transversely, as discussed in the previous section) we obtain the following $2N \times 2N$ transfer matrix (for $N \geqslant 2$)

$$\hat{T} = \frac{1}{2\mathrm{i}\sin kl}\begin{pmatrix} \mathrm{e}^{2\mathrm{i}kl}\hat{1}_N + \mathrm{e}^{2\mathrm{i}kl}\hat{\Omega} & \mathrm{e}^{-2\mathrm{i}kl}\hat{1}_N + \hat{\Omega} \\ -\hat{1}_N - \mathrm{e}^{2\mathrm{i}kl}\hat{\Omega} & (1-2\mathrm{e}^{-2\mathrm{i}kl})\hat{1}_N - \hat{\Omega} \end{pmatrix} \tag{10}$$

with $\hat{1}_N$ denoting the $N \times N$ identity matrix, and with $\hat{\Omega}$ being an $N \times N$ submatrix of the form

$$\hat{\Omega} = \begin{pmatrix} 0 & -\mathrm{e}^{-\mathrm{i}kl} & 0 & 0 & 0 & \ldots & 0 \\ -\mathrm{e}^{-\mathrm{i}kl} & 1 & -\mathrm{e}^{-\mathrm{i}kl} & 0 & 0 & \ldots & 0 \\ 0 & -\mathrm{e}^{-\mathrm{i}kl} & 1 & -\mathrm{e}^{-\mathrm{i}kl} & 0 & \ldots & 0 \\ 0 & . & . & . & . & . & 0 \\ 0 & . & . & . & . & . & 0 \\ 0 & 0 & 0 & . & -\mathrm{e}^{-\mathrm{i}kl} & 1 & -\mathrm{e}^{-\mathrm{i}kl} \\ 0 & 0 & 0 & . & 0 & -\mathrm{e}^{-\mathrm{i}kl} & 0 \end{pmatrix}. \tag{11}$$

Hence the total transfer matrix of a finite piece of a square network of 'width' N and 'length' M will be a product of M matrices of the form (10). This matrix summarizes the full information of multiple splittings and can give all the transmission properties of this network under this type of boundary conditions. (We will see below, however, that a simple choice of width $N = 2$ and length $M = 2$ (equivalent to a single unit cell) is sufficient to exhibit resonance phenomena related to properties of the infinite square network.)

(ii) For periodic boundary conditions along the transverse direction, namely $C_N = C_0\,\mathrm{e}^{\mathrm{i}N\phi}$ and $D_N = D_0\,\mathrm{e}^{\mathrm{i}N\phi}$ we obtain the corresponding $2N \times 2N$ result (again for $N \geqslant 2$)

$$\hat{T} = \frac{1}{2\mathrm{i}\sin kl}\begin{pmatrix} 2\mathrm{e}^{2\mathrm{i}kl}\hat{1}_N - \mathrm{e}^{\mathrm{i}kl}\hat{\Omega}' & (1+\mathrm{e}^{-2\mathrm{i}kl})\hat{1}_N - \mathrm{e}^{-\mathrm{i}kl}\hat{\Omega}' \\ -(1+\mathrm{e}^{2\mathrm{i}kl})\hat{1}_N + \mathrm{e}^{\mathrm{i}kl}\hat{\Omega}' & -2\mathrm{e}^{-2\mathrm{i}kl}\hat{1}_N + \mathrm{e}^{-\mathrm{i}kl}\hat{\Omega}' \end{pmatrix} \tag{12}$$

with $\hat{\Omega}'$ again being an $N \times N$ submatrix, but now of the form

$$\hat{\Omega}' = \begin{pmatrix} 0 & 1 & 0 & \ldots & \mathrm{e}^{-\mathrm{i}\phi} \\ 1 & 0 & 1 & \ldots & 0 \\ 0 & 1 & 0 & \ldots & 1 \\ . & . & . & . & . \\ . & . & . & . & . \\ \mathrm{e}^{\mathrm{i}\phi} & 0 & 1 & \ldots & 0 \end{pmatrix} \tag{13}$$

and once again the total transfer matrix of a finite piece of a square network ($N \times M$) will be a product of M matrices of the form (12).

We make the following important observation for case (i): if we take just a double vertex ($N = 2$), the transfer matrix associated with the unit cell of the square network (hence $M = 2$ as well) is just the square of matrix (10). This matrix has off-diagonal elements proportional to $\cot kl$, which are therefore vanishing for $kl = (2\rho + 1)(\pi/2)$. These 'resonances' that are observed for the *single* unit cell under 'free scattering' boundary conditions, correspond, as we will show below, to a special property of the bands of the *infinite* square network and they are related to states that are 'maximally extended' (see the next subsection). Hence the finite (even small, with just a single unit cell) transmission problem, for this type of boundary conditions, carries the memory of the most extended states (in the thermodynamic limit) in the form of the vanishing of appropriate partial reflection coefficients. This motivates the treatment of a single unit cell of a somewhat more complex network in section 4.

3.2. Band structure

Let us actually find the exact band structure of an (infinite) square network: this results from relating coefficients periodically in both orthogonal directions. By identifying, for example, the coefficients in the single-vertex system ($N = M = 1$) (see figure 1(*c*)) in the following way

$$A_1' = A_1 e^{i\phi_1} \qquad B_1' = B_1 e^{i\phi_1}$$

and

$$A_0' = A_0 e^{i\phi_2} \qquad B_0' = B_0 e^{i\phi_2}$$

all eight coefficients appearing in this problem can be eliminated, with a resulting relation between kl and ϕ_1 and ϕ_2. This relation is the exact band structure (since k is related to the energy E by $k^2 = 2mE/\hbar^2$), and the two phases define the crystal momenta (q_1 and q_2) in the two orthogonal directions through $\phi_1 = q_1 l$ and $\phi_2 = q_2 l$. The resulting band structure is

$$\frac{2m}{\hbar^2} El^2 = [\arccos(\tfrac{1}{2}\cos q_1 l + \tfrac{1}{2}\cos q_2 l)]^2. \tag{14}$$

Plotting (14) for $q_1 l$ as a function of E (for several fixed values of $q_2 l$), we see gaps opening at regions where $q_1 l$ becomes a complex number (figure 2). (We also observe a manifestation of the Higgs mechanism (i.e. the opening of a gap at $E = 0$) that is further discussed in the next section.) It is interesting that, by smoothly changing $q_2 l$ we see that the band structure is actually *moving*. This is an additional feature (of coupling between the two modes) in comparison to standard tight-binding band structures. Note, however, that during this movement, there are some special points in k-space given by $kl = (2\rho + 1)(\pi/2)$ that *always* lie in bands (and they are the only points that have this property), see figure 2. This shows that these points label what could be called 'maximally extended' states. Recall that these are the points that give 'resonances' (vanishings of the partial reflection coefficients) in the 'free-scattering' transfer matrices of a *single* unit cell. This motivates our later proposition that a resonance that we will find in a non-trivial network, under introduction of a defect, may also be related to the possible creation of extended states. (Spectral properties of a more general rectangular lattice have been discussed recently [8], with emphasis on incommensurability issues with respect to the ratio of the two lattice constants.)

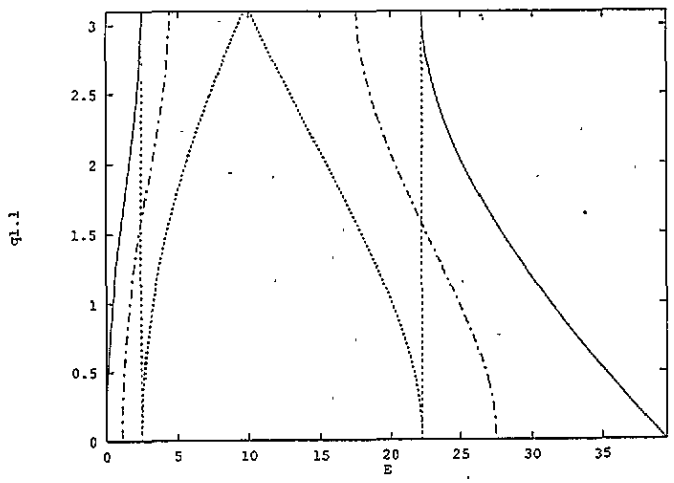

Figure 2. Movement of the band structure of a square network as $q_2 l$ is varied. The solid curve corresponds to $q_2 l = 0$, the dashed-dotted curve to $q_2 l = \pi/2$, and the dotted curve to $q_2 l = \pi$. The two vertical lines show the positions of two special energies corresponding to $kl = \pi/2$ and $kl = 3\pi/2$. Note that these points *always* belong to a band. (Units $(2m/\hbar^2)l^2 = 1$ are used.)

4. A low 2D Penrose approximant

4.1. Transmission problem

The simplest way of filling the plane periodically with the standard two Penrose rhombic tiles is shown in figure 3(*a*) (where the two linearly independent directions are also shown, labelled by the two phases ϕ_1 and ϕ_2 that will later enter into the band structure). This structure can be viewed as a low 2D Penrose approximant.

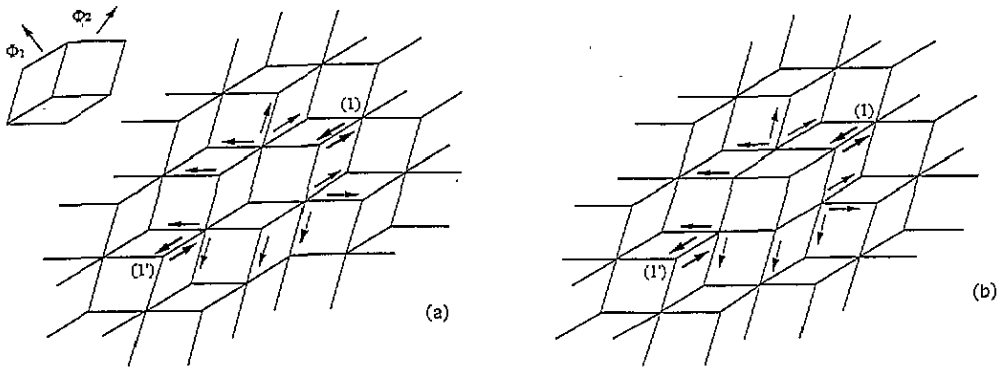

Figure 3. (a) A low 2D approximant network. There are three directions along which the unit cell is repeated; two of them are independent and are symbolized by the phases ϕ_1 and ϕ_2 (the third is then described by the phase $\phi_1 - \phi_2$). A single unit cell is shown in the centre, with arrows in the 'outside branches' (which are determined by filling the plane with periodic repetition of this unit cell in all three directions). Single arrows signify 'free scattering' boundary conditions (see the text at the beginning of section 4). 1 and 1′ denote the input and output branches (where reflections are allowed). (*b*) The result of flipping the interior of the central unit cell, but keeping the external environment the same.

Let us determine the transfer matrix for the scattering of electrons through a single unit cell of such an ordered system, by treating branch 1 as the input branch, and 1′ as the output one (see figure 3(*a*)). All other 'outside' branches shown in figure 3(*a*) are treated as transverse escapes. Let us therefore apply 'free scattering' boundary conditions for these escape wires (that are ten in number). It turns out that we now have 30 matching equations overall (describing the complete physics at the seven vertices). The total number of branches is 21 (which means 42 coefficients overall), and since from the boundary conditions ten of them vanish, we can solve this linear system of equations for $(42-10)-30=2$ quantities (i.e. A_1' and B_1'), a procedure which indeed yields a 2×2 transfer matrix (linearly relating A_1', B_1' with A_1, B_1) as claimed earlier. The above procedure is actually equivalent to inverting a 30×30 matrix, in order to obtain the final 2×2 transfer matrix for this problem. This 30×30 matrix carries the full memory of the structure of the unit cell (through the particular connectivities), *both* the internal structure, and *also* the external connectivities as well (recall from the earlier discussion in section 2 that this was crucial for the form of the resulting matrix).

The transfer matrix that results from this procedure gives, through equations (8) and (9), the following exact results for the reflection and transmission coefficients

$$R=\frac{1}{9}\frac{31\,913+39\,744\cos 2kl+8343\cos 4kl}{5897+6336\cos 2kl+567\cos 4kl} \tag{15}$$

and

$$T=\frac{128}{9}\frac{13+12\cos 2kl}{5897+6336\cos 2kl+567\cos 4kl}. \tag{16}$$

Note that R has a maximum for $kl=(2\rho+1)(\pi/2)$. This is actually related to the fact that for the infinite approximant, these points correspond to the middle of gaps, as will be seen below (subsection 4.2). Indeed for an infinite strip of such (ordered) units parallel to the 11′ direction (i.e. in such a way as to have the output of one as the input of another), the total transfer matrix is an infinite product of elementary transfer matrices, and the corresponding (12)-element will diverge; a reflection coefficient that goes to infinity indeed signifies the presence of a gap.

What is, however, more interesting is the problem of a unit with a 'flipped' internal structure (while keeping the external connectivities *the same*, to simulate the fact that the flipping is in the interior of *only* one unit cell and not in the external environment). This 'flipped' system is shown in figure 3(*b*). By going through the new matching equations and inverting the new 30×30 matrix we obtain the following exact results

$$R=\frac{4(\cos kl)^2}{9}\frac{12\,781+8299\cos 2kl-180\cos 4kl-900\cos 6kl}{6821+6284\cos 2kl+255\cos 4kl-460\cos 6kl-100\cos 8kl} \tag{17}$$

and

$$T=\frac{128}{9}\frac{17+8\cos 2kl}{6821+6284\cos 2kl+255\cos 4kl-460\cos 6kl-100\cos 8kl}. \tag{18}$$

From the structure of (17) we see that for the special points $kl=(2\rho+1)(\pi/2)$ (where the ordered system was found to have a maximum) the reflection coefficient *vanishes rigorously*. This vanishing is a very special situation that does not happen in the ordered system. It shows that if we put any finite number of flipped units in an otherwise ordered strip, the resistance will go down. Even more spectacular is the fact that even an infinite strip of flipped units along this special symmetry direction will have a vanishing total reflection coefficient (due to the vanishing of the (12)-element of each transfer matrix, any product of these matrices, even an infinite number of them, will have a (12)-element that will also be rigorously vanishing). The reflection coefficients (15) and (17) are plotted in figure 4.

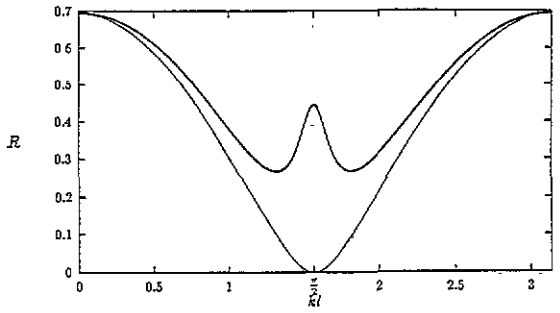

Figure 4. The reflection coefficients, equations (15) and (17), for the units shown in figures 3(*a*) and (*b*). Unit 3(*a*) shows a local maximum, and unit 3(*b*) shows a vanishing at the special point $kl = \pi/2$.

4.2. Band structure

Let us now determine the band structure of the ordered infinite approximant network. We relate coefficients, through a phase ϕ_1 or ϕ_2 or $\phi_1 - \phi_2$, for corresponding branches of unit cells that repeat in the three possible directions. An example is shown in figure 5, showing connections through phases ϕ_1 and ϕ_2. The final result comes, after elimination of all coefficients, from a 12×12 determinant, and is

$$\frac{2m}{\hbar^2} El^2 = \left[\tfrac{1}{2} \arccos\left(\frac{(-3 + 4\cos\phi_1 + 4\cos\phi_2 + 4\cos(\phi_1 - \phi_2)}{9}\right)\right]^2. \tag{19}$$

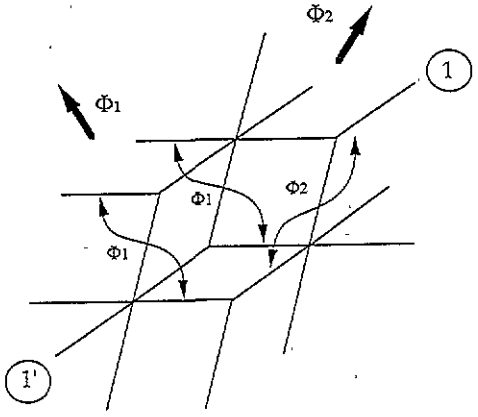

Figure 5. An example of how to relate coefficients through ϕ_1 and ϕ_2, in order to determine analytically the band structure of an infinite network with the unit cell of figure 3(*a*).

This exact and analytically given band structure is plotted in figure 6 (for fixed ϕ_2). We see again the gap structure opening at regions where ϕ_1 becomes a complex quantity. Once again we observe gaps in the origin, which is a manifestation of the Higgs mechanism: this is expected for *any* network because even in the long-wavelength limit the space is full of 'holes' and never homogeneous, resulting in the disappearance of Goldstone modes and the opening of a gap at the origin.

A contour plot $E(\phi_1, \phi_2)$ of (19) (surfaces of constant energy) is also given in figure 7. This shows the possible 'Fermi surfaces', if the incidence energy is identified, as usually done, with the Fermi energy. (For free particles in full 2D space we would of course have homocentric circles.)

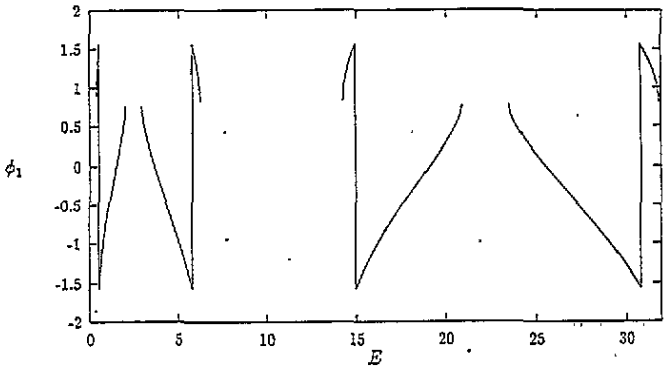

Figure 6. The band structure of an infinite network with the unit cell of figure 3(*a*) (for $\phi_2 = \pi/2$). Gaps open at regions where ϕ_1 becomes a complex number.

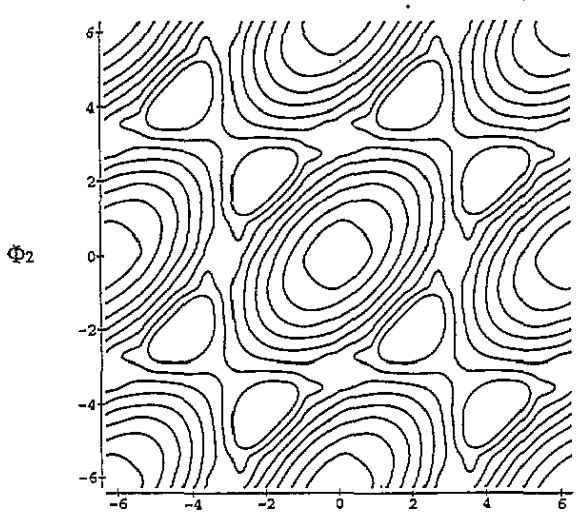

Figure 7. The possible Fermi surfaces associated with the network with the unit cell of figure 3(*a*).

Note from the band structure (19), that the resonance upon flipping found above is *always* in the middle of gaps of the ordered system. If the resonance is indeed a demonstration of the extendedness of states (as it is in the case of a square network discussed earlier), one interpretation would be that new levels may be created in some gaps of the ordered system upon introduction of the phason defect. This is in agreement with numerical findings for a 2D Penrose system [4] in a tight-binding model.

We finally report that a calculation for a much bigger unit (that consists of a central unit cell together with all six neighbouring unit cells, see figure 8) gives the result plotted in figure 8. We note that a very deep minimum close to zero is also observed in the case when we only flip the central unit cell, whereas a very pronounced maximum appears in the ordered (unflipped) system.

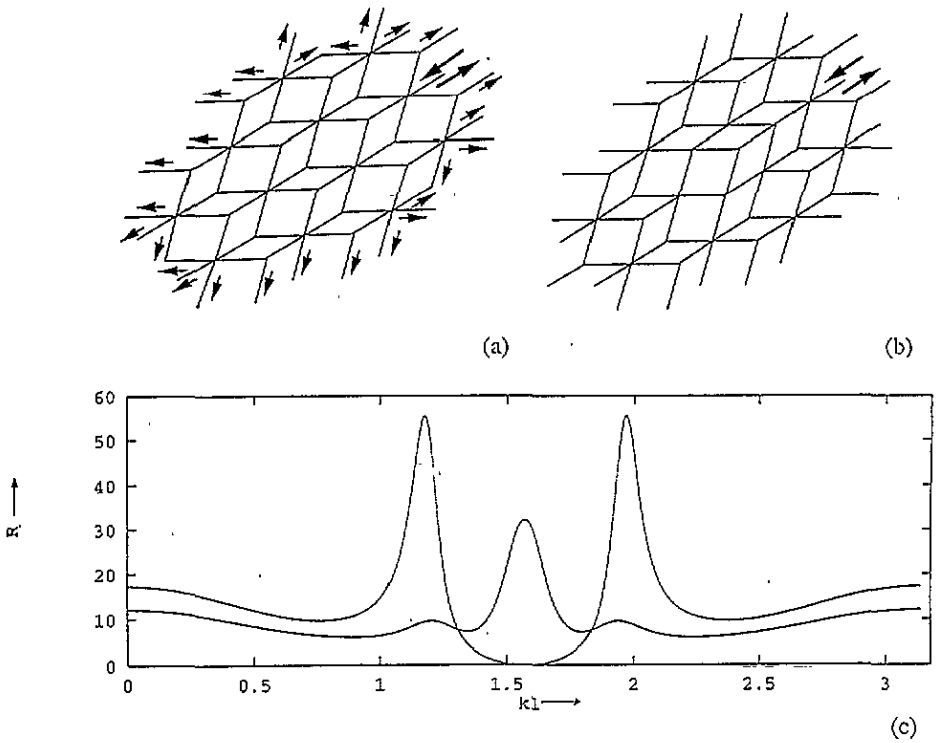

Figure 8. The reflection coefficients (c) for a bigger central unit (a), consisting of seven unit cells (one central and the six neighbouring ones). For the ordered (unflipped) system (a) we observe a local maximum; for the system with a flipped central unit cell (b), we observe a deep minimum very close to zero ($R_{min} = 0.017$), at $kl = \pi/2$.

5. A 3D Penrose approximant network

We now search for the above resonance phenomena in a more complex three-dimensional Penrose network, with a unit cell consisting of four rhombohedra of two types, as shown in figure 9(a). It turns out that the problem is richer [9] than the corresponding 2D network, but in one case we indeed observe the same type of resonance upon flipping of the internal rhombohedra (see figure 9(b)), but again keeping the external connectivities the same. This result is shown in figure 9(c), where the reflection coefficients of the ordered and the flipped system are compared.

6. Conclusion

We have found a vanishing reflection coefficient for a strip of flipped units in a 2D and also in a 3D network of wires for special incidence energies. The first obvious question is whether this type of resonance is experimentally detectable. With recent advances in microfabrication techniques extremely narrow wires can actually be manufactured. (Experiments in quasiperiodic superconducting networks [10] have already been performed.) Alternatively, one can try the analogous acoustic experiments [11] to observe the above phenomena. What is required for these types of resonances to be observed, is reflectionless reservoirs in the transverse channels, so that the 'free scattering' boundary conditions are

satisfied.

From a theoretical point of view and in relation to quasicrystalline approximants, we have argued that the above resonances may be related to the possible creation of extended states, upon flipping, in the gaps of the ordered system. If this is true, it may be seen as a possible mechanism of lowering the resistance with the introduction of defects, a tendency that is in general agreement with real experiments [1] on approximants and with numerical treatments [4].

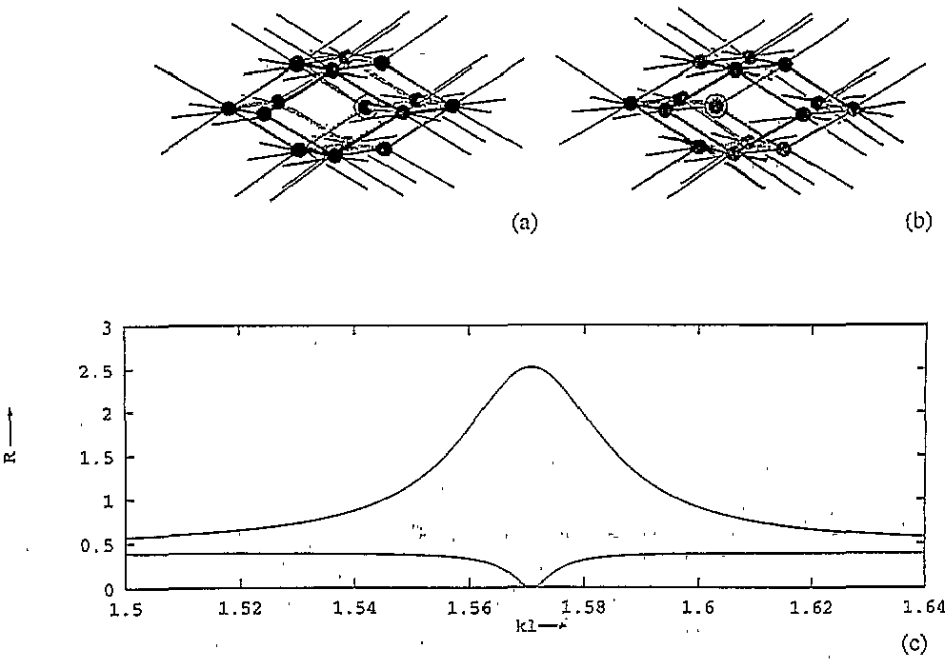

Figure 9. (*a*) The unit cell of a low 3D approximant. (*b*) The corresponding unit with 'flipped' internal structure (but the same external environment). (*c*) The corresponding reflection coefficients showing a vanishing for the flipped system at the same special point $kl = \pi/2$.

We should also emphasize that the above results are rigorously valid for a low-periodic approximant. Whether they persist in cases of more complex unit cells, and ultimately in the limiting case of a quasicrystal (an infinite size unit cell) is not known and deserves further investigation.

Finally, from an academic point of view, the above model systems are rare (if not unique) examples of exactly soluble band structures in high dimensionality. Furthermore, using these exact band structures as 'input' one can go further in building a semiclassical dynamics [12] to study time-dependent propagation in these networks. Effects of disorder can also be studied through the introduction of random potentials as already mentioned. Finally, the introduction of a magnetic field is possible (and the problem is still soluble). This can address questions related to the quantum Hall effect [13] in quasicrystalline approximants, a subject that is still open to investigation.

Acknowledgment

One of us (KM) acknowledges support from the European Union through the Human Capital and Mobility Program.

Appendix

We here derive equation (7) for the effective resistance of a system in the case where electrons can also escape or be incident in transverse directions. Consider figure 1(*c*). Imagine that the system under consideration is located at the position of the vertex. Then view wire 1 as the input and wire 1′ as the output wire. Channels 0 and 0′ are to be taken as the transverse channels (see text). We now modify the standard Landauer argument [7] to this more general case.

Suppose that we apply a potential difference δV between 1 and 1′. This creates a density change

$$\delta n = \frac{\mathrm{d}n}{\mathrm{d}E} e\,\delta V. \tag{20}$$

This change can also be written as

$$\delta n = \left(|A_1|^2 + |B_1|^2\right) - \left(|A_1'|^2 + |B_1'|^2\right) \tag{21}$$

in terms of the plane wave coefficients shown in figure 1(*c*).

The input current in channel 1 is

$$I_1 = ev\left(|A_1|^2 - |B_1|^2\right) \tag{22}$$

while the output current in channel 1′ is

$$I_1' = ev\left(|A_1'|^2 - |B_1'|^2\right) \tag{23}$$

where it is assumed that the Fermi velocity $v = \partial E/\partial k$ is the same in both sides. Here we will *not* assume the usual 1D conservation of current $I_1 = I_1'$, because of the presence of channels 0 and 0′. Let us call the 'effective resistance' the ratio

$$\mathcal{R} = \frac{\delta V}{I_1}. \tag{24}$$

Using (20), (21) and (22) we obtain

$$\mathcal{R} = \frac{\mathrm{d}E/\mathrm{d}n\left[\left(|A_1|^2 + |B_1|^2\right) - \left(|A_1'|^2 + |B_1'|^2\right)\right]}{e^2 v\left(|A_1|^2 - |B_1|^2\right)}. \tag{25}$$

The total reflection and transmission coefficients for this system are given by

$$R = \frac{|B_1|^2 - |B_1'|^2}{|A_1|^2 - |B_1'|^2} \tag{26}$$

and

$$T = \frac{|A_1'|^2 - |B_1'|^2}{|A_1|^2 - |B_1'|^2}. \tag{27}$$

From (26) and (27) it turns out that

$$|A_1|^2 - |B_1|^2 = T\left(|A_1|^2 - |B_1'|^2\right) - \delta I \tag{28}$$

and

$$\left(|A_1|^2+|B_1|^2\right)-\left(|A_1'|^2+|B_1'|^2\right)=2R\left(|A_1|^2-|B_1'|^2\right)-\delta I \tag{29}$$

with the definition

$$\delta I=|A_0|^2-|B_0|^2-|A_0'|^2+|B_0'|^2. \tag{30}$$

The notation manifests the fact that this quantity is related to the current change. Indeed, conservation of the *total* number of electrons (*including* the ones incident or escaping through the transverse channels) gives

$$|A_1|^2-|B_1|^2+|A_0|^2-|B_0|^2=|A_1'|^2-|B_1'|^2+|A_0'|^2-|B_0'|^2 \tag{31}$$

which in turn, through the use of (22) and (23) leads to

$$\delta I=\frac{1}{ev}\left(I_1'-I_1\right). \tag{32}$$

Finally, in a standard transmission problem we set $B_1'=0$, so that $|A_1'|^2=T|A_1|^2$ and $|B_1|^2=R|A_1|^2$. This leads to

$$\delta I=(T+R-1)\,|A_1|^2. \tag{33}$$

Substituting (28), (29) and (33) into (25), and with

$$\frac{\mathrm{d}E}{\mathrm{d}n}=\frac{\partial E/\partial k}{\partial n/\partial k}=\frac{v}{2/\pi\hbar}$$

for a 1D system and for spin-$\frac{1}{2}$ electrons, we obtain equation (7). The standard Landauer result R/T follows in the special case $\delta I=0$, which is equivalent to $R+T=1$.

References

[1] For a review, see C Berger in 1994 *Lectures On Quasicrystals* ed F Hippert and D Gratias (Paris: Les Editions de Physique Les Ulis)

[2] Moulopoulos K and Roche S *Phys. Rev.* B to be published

[3] Exner O P and Seba P 1989 *Rep. Math. Phys.* **27** 7
Avron J E and Sadun L 1989 *Phys. Rev. Lett.* **62** 3082
Avishai Y and Luck J M 1992 *Phys. Rev.* B **45** 1074

[4] Fujiwara T, Yamamoto S and Trambly de Laissardiere G 1993 *Phys. Rev. Lett.* **71** 4166

[5] de Gennes P G 1981 *C. R. Acad. Sci.* B **292** 279
Alexander S 1983 *Phys. Rev.* B **27** 1541

[6] Langreth D C and Abrahams E 1981 *Phys. Rev.* B **24** 2978

[7] Landauer R 1970 *Phil. Mag.* **21** 863

[8] Exner P 1995 *Phys. Rev. Lett.* **74** 3503

[9] Moulopoulos K unpublished

[10] Pannetier B *et al* 1984 *Phys. Rev. Lett.* **53**, 1845
Behrooz A *et al* 1986 *Phys. Rev. Lett.* **57** 368
Itzler M A *et al* 1993 *Phys. Rev.* B **47** 14165

[11] He S and Maynard J D 1989 *Phys. Rev. Lett.* **62** 1888

[12] Ashcroft N W and Mermin N D 1976 *Solid State Physics* (New York, Philadelphia: Holt-Saunders) ch 12

[13] See Kohmoto M 1993 *J. Phys. Soc. Japan* **62** 4001